



Applied Mathematics and Nonlinear Sciences

<https://www.sciendo.com>

Effects of second-order slip and drag reduction in boundary layer flows

Kuppalapalle Vajravelu^{1†}, Ronald Li¹, Mangalagama Dewasurendra¹, Joseph Benarroch¹, Nicholas Ossi¹, Ying Zhang¹, Michael Sammarco¹, K.V. Prasad²

¹Department of Mathematics, University of Central Florida, Orlando, FL 32816-1364, USA

²Department of Mathematics, VSK University, Vinayaka Nagar, Bellary-583 104, Karnataka, India

Submission Info

Communicated by Juan L.G. Guirao

Received 24th March 2018

Accepted 17th June 2018

Available online 17th June 2018

Abstract

In this paper, boundary layer flow over a moving flat plate with second-order velocity slip, injection and applied magnetic field is analyzed. The governing partial differential equations are converted in to a nonlinear ordinary differential equation through an appropriate similarity transformation. The resulting nonlinear equation is solved via homotopy analysis method (HAM). Errors ranging from 10^{-7} to 10^{-10} are reported for a relatively few terms. The effects of the pertinent parameters on the velocity and the shear stress are presented graphically and discussed. In the absence of magnetic field and the two slip parameters, the results are found to be in excellent agreement with the available results in the literature. It is expected that the results obtained will not only provide useful information for industrial applications but also complement the earlier works.

Keywords: Second-order slip, drag reduction, boundary-layer flow, homotopy analysis method.

AMS 2010 codes: 65L10, 76D10.

1 Introduction

As we know, a moving flat plate in a fluid medium infuses a boundary layer. This kind of flow appears in several technological industries, such as extrusion process, wire and fiber coating, polymer processing, food-stuff processing, design of heat exchangers, and chemical processing equipment. The pioneering work of Sakiadis [1, 2] on the laminar boundary layer over a rigid surface moving in its own plane is quite different from the flow past a stationary surface (known as the classical Blasius [3] flow). Tsou et al. [4] examined the results of Sakiadis [2], analytically and experimentally, which includes both laminar and turbulent flow conditions. Vajravelu and Mohapatra [5] investigated the effects of injection, analytically, on the boundary layer flow past a moving sheet. Takhar et al. [6] analyzed the boundary layer flow due to a moving plate in the presence

[†]K. Vajravelu.

Email address: kuppalapalle.vajravelu@ucf.edu

of variable fluid properties. Furthermore, Andersson and Aarseth [7] revisited the Sakiadis flow problem with the view to assess some crucial misconceptions of the flow behavior and provided numerical results for water at atmospheric pressure. Ahmad et al. [8] extended the Blasius and Sakiadis problems to nanofluids. Ding and Xin [9] used fixed-point method (FPM) and obtained semi-analytical solutions for classical Blasius flow. In recent years, several authors examined the boundary layer flow a past moving sheet or stretching sheet by considering Newtonian/non-Newtonian fluids with various constraints (Vajravelu et al. [10] and Prasad et al. ([11]- [13])).

The velocity slip is a phenomenon of non-adherence of the fluid to a solid boundary. More often "apparent wall slip" occur at solid boundaries for the fluids like slurries, gels, emulsions, and foam. Even for these fluids, equations of motion are governed by Navier-Stokes equations with no-slip condition. Beavers and Joseph [14], introduced the concept of a slip flow condition at the boundary. In view of this, Andersson [15] and Wang [16] considered Newtonian fluid flow past a linearly stretching sheet under partial slip (first order slip/general slip) condition. Many researchers such as Fang et al. [17], Sajid et al. [18], Matthews and Hill [19] considered partial slip in the absence of heat transfer, whereas Hayat et al. [20], Yazdi et al. [21], Sahoo [22] considered both partial slip and heat transfer character. Also, for further applications see Zhu et al. [23], Mansur et al. [24], Zhu et al. [25], Sahoo et al. [26] and Hayat et al. [27]. The Maxwell [28] slip condition is widely accepted and implemented in current rarefied gas flow. However, the Maxwell model is only applicable for the gas flows where the rarefaction and roughness effects are not evident. Beskok and Karniadakis [29] proposed a classical second-order slip boundary condition and used it to solve the Navier-Stokes equations for confined fluids at the microscale and nanoscale. Wu [30] explored a new and advanced second-order slip velocity model. Fang et al. [31] used this model to obtain exact solutions of the governing Navier-Stokes equations.

In view of these applications, the problem studied here extends the work of Vajravelu and Mohapatra [5] to the second-order slip velocity at a moving plate. The coupled non-linear partial differential equations governing the problem are transformed into a system of coupled non-linear ordinary differential equations. The transformed equations are solved analytically via homotopy analysis method (HAM). Computed results for the flow characteristics are analyzed. The analysis of the results shows that the fluid flow is appreciably influenced by the sundry parameters. It is expected that the results obtained will not only provide useful information for industrial applications but also complement the earlier works.

2 Mathematical formulation

Consider a flow of an incompressible viscous fluid, with constant velocity U_∞ past a parallel, porous, semi-infinite flat plate moving with a constant velocity U_w in the direction opposite to the main stream (see Fig.1, not drawn to scale). Let the x -axis be taken along the plate, with positive x being the direction of the flow, and the y -axis is normal to it. Further, let the fluid properties be constant. Under these assumptions, the governing boundary-layer equations for the flow are

$$\frac{\partial u}{\partial x} + \frac{\partial v}{\partial y} = 0, \quad (1)$$

$$u \frac{\partial u}{\partial x} + v \frac{\partial u}{\partial y} = \nu \frac{\partial^2 u}{\partial y^2} - \frac{\sigma B_0^2}{\rho 2x} (u - U_\infty), \quad (2)$$

where ν is the kinematic viscosity of the fluid and the other symbols have their usual meanings. The appropriate boundary conditions are

$$u = -(U_w + U_{Slip}), \quad v = v_w(x) = C \sqrt{\frac{\nu U_\infty}{2x}} \quad \text{at } y = 0, \quad u = U_\infty \quad \text{as } y \rightarrow \infty. \quad (3)$$

where u and v are the velocity components in the x - and y -directions, respectively, and U_{Slip} is the slip velocity at the wall. Wu's [30] slip velocity model (valid for arbitrary Knudsen numbers K_n) is given by

$$U_{Slip} = \frac{2}{3} \left(\frac{3 - \alpha l^3}{\alpha} - \frac{3}{2} \frac{1 - l^2}{K_n} \right) \lambda(x) \frac{\partial u}{\partial y} - \frac{1}{4} \left(l^4 + \frac{2}{K_n^2} (1 - l^2) \right) \lambda^2(x) \frac{\partial^2 u}{\partial y^2} = A \lambda(x) \frac{\partial u}{\partial y} + B \lambda^2(x) \frac{\partial^2 u}{\partial y^2} \quad (4)$$

where $l = \min[1/K_n, 1]$, α is the momentum accommodation coefficient with $0 \leq \alpha \leq 1$, and $\lambda(x) = \lambda x^{1/2}$ is the molecular mean free path. The molecular mean free path is always positive. Thus, $B < 0$, and hence the second term in right hand side of Eq.(4) is positive. There are numerous applications that involve micro-scale devices including sensors, heat exchangers, and micro-power systems. Based on Knudsen number (K_n), Beskok and Karniadakis [29] classified the gas flow in micro channels into four flow regimes: (a) continuum flow regime ($K_n \leq 0.001$) (b) slip flow regime ($0.001 \leq K_n \leq 0.1$); (c) transition flow regime ($0.1 \leq K_n \leq 10.0$) and (d) free molecular flow regime ($K_n > 10$).

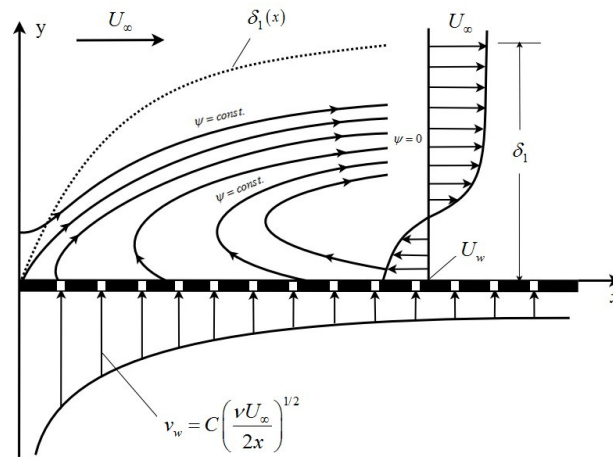


Fig. 1 Physical model with coordinate system. δ_1 represents the thickness of the boundary layer

The stream function and the similarity variables can be written as

$$\eta = \sqrt{\frac{U_\infty}{2\nu x}} y, \quad \psi(x, y) = \sqrt{2\nu x U_\infty} f(\eta). \quad (5)$$

Now, the velocity components can be expressed as

$$u = U_\infty f'(\eta), v = -\sqrt{\frac{\nu U_\infty}{2x}} [f(\eta) - \eta f'(\eta)]. \quad (6)$$

Hence, the mass transfer velocity at the wall becomes

$$v_w(x) = -\sqrt{\frac{\nu U_\infty}{2x}} f(0). \quad (7)$$

Using (5) and (6) in equations (1)-(3), we get

$$f''' + f f'' - Mn(f' - 1) = 0 \quad (8)$$

with the boundary conditions

$$f(0) = -C, \quad f'(0) = -\lambda_1 - \gamma f''(0) - \delta f'''(0), \quad f' \rightarrow 1 \text{ as } \eta \rightarrow \infty, \quad (9)$$

where C is the wall mass transfer parameter, $\lambda_1 = \frac{U_w}{U_\infty}$ is the velocity ratio parameter, γ is the first-order velocity slip parameter with $0 < \gamma = A\sqrt{\frac{U_\infty}{2\nu}}$ and δ is the second-order velocity slip parameter with $0 > \delta = B\frac{U_\infty}{2\nu}$ and $Mn = \frac{\sigma B_0^2}{\rho U_\infty}$ is the magnetic parameter.

The physical quantity of interest is the skin friction coefficient C_f which takes the form

$$C_f = \frac{\tau_{wx}}{\rho U_w^2}, \quad (10)$$

where τ_w is the wall skin friction, given by

$$\tau_w = \mu \left(\frac{\partial u}{\partial y} \right)_{y=0}. \quad (11)$$

From Eq.(5), the dimensionless skin friction coefficient becomes

$$\sqrt{\frac{Re}{2}} C_f = f''(0), \quad (12)$$

where $Re = \frac{U_x}{\nu}$ is the local Reynolds number.

3 Analytic solution via homotopy analysis method

For obtaining solution to the problem, we turn to homotopy analysis method (HAM). In 1992, Liao proposed HAM to serve as a general analytical method for solving nonlinear problems [32]. The accuracy and robustness of the HAM for solving nonlinear boundary value problems has been repeatedly confirmed in a wide range of papers, including: Lane-Emden equation [33], time-dependent Michaelis-Menton equation [34], non-local Whitham equation [35], and Zakharov system [36] to name a few. Here we outline the solution method and later discuss the convergence and accuracy of the HAM solution.

For the present problem, we choose the auxiliary linear operator \mathcal{L} as

$$\mathcal{L} = \frac{\partial^3}{\partial \eta^3} + \beta \frac{\partial^2}{\partial \eta^2}, \quad (13)$$

with an initial approximation to $f(\eta)$ as

$$f_0(\eta) = \eta + \frac{\lambda_1 + 1}{\beta - \gamma\beta^2 + \delta\beta^3} e^{-\beta\eta} - \left(C + \frac{\lambda_1 + 1}{\beta - \gamma\beta^2 + \delta\beta^3} \right), \quad (14)$$

where $\beta > 0$ is a convergence control parameter to be chosen later. From Eq.(8), we define the nonlinear operator \mathcal{N} as

$$\mathcal{N}[\hat{f}(\eta, q, \hbar, \beta)] = \frac{\partial^3 \hat{f}(\eta, q, \hbar, \beta)}{\partial \eta^3} + \hat{f}(\eta, q, \hbar, \beta) \frac{\partial^2 \hat{f}(\eta, q, \hbar, \beta)}{\partial \eta^2} - Mn \left(\frac{\partial \hat{f}(\eta, q, \hbar, \beta)}{\partial \eta} - 1 \right). \quad (15)$$

The so-called zeroth-order deformation equation is

$$(1 - q)\mathcal{L}[\hat{f}(\eta, q, \hbar, \beta) - f_0(\eta)] - q\hbar\mathcal{N}[\hat{f}(\eta, q, \hbar, \beta)] = 0, \quad (16)$$

with boundary conditions

$$\hat{f}(0, q, \hbar, \beta) = -C, \quad \hat{f}'(0, q, \hbar, \beta) = -\lambda_1 - \gamma\hat{f}''(0, q, \hbar, \beta) - \delta\hat{f}'''(0, q, \hbar, \beta), \quad \hat{f}'(\infty, q, \hbar, \beta) = 1, \quad (17)$$

where $q \in [0, 1]$ is the embedding parameter, $\hbar \neq 0$ is a convergence control parameter, and the prime denotes differentiation with respect to η . At $q = 0$ and $q = 1$, we get respectively

$$\widehat{f}(\eta, 0, \hbar, \beta) = f_0(\eta), \quad \text{and} \quad \widehat{f}(\eta, 1, \hbar, \beta) = f(\eta). \quad (18)$$

Therefore, as q increases from 0 to 1, $\widehat{f}(\eta, q, \hbar, \beta)$ varies continuously from the initial approximation $f_0(\eta)$ to the solution of interest $f(\eta)$. By defining

$$f_m(\eta, \hbar, \beta) = \frac{1}{m!} \left. \frac{d^m f(\eta, q, \hbar, \beta)}{dq^m} \right|_{q=0} \quad (19)$$

we expand $\widehat{f}(\eta, q, \hbar, \beta)$ about q to obtain

$$\widehat{f}(\eta, q, \hbar, \beta) = f_0(\eta) + \sum_{m=1}^{\infty} f_m(\eta, \hbar, \beta) q^m. \quad (20)$$

With prudent choice of the auxiliary linear operator, initial approximation, and convergence control parameters, the series in (20) can be made convergent at $q = 1$. The HAM series solution now becomes

$$f(\eta) = f_0(\eta) + \sum_{m=1}^{\infty} f_m(\eta, \hbar, \beta) \quad (21)$$

In order to obtain $f_m(\eta, \hbar, \beta)$, we differentiate Eq. (16) m times with respect to q , divide by $m!$, and finally evaluate at $q = 0$ to arrive at the so-called m^{th} -order deformation equation

$$\mathcal{L}[f_m(\eta, \hbar, \beta) - \chi_m f_{m-1}(\eta, \hbar, \beta)] = \hbar \left[f_{m-1}''' + \sum_{n=0}^{m-1} f_{m-1-n} f_n'' - \text{Mn}(f_{m-1}') + \text{Mn}(1 - \chi_m) \right], \quad (22)$$

with corresponding boundary conditions

$$f_m(0, \hbar, \beta) = 0, \quad f_m'(0, \hbar, \beta) = 0, \quad \text{and} \quad f_m'(\infty, \hbar, \beta) = 0, \quad (23)$$

where χ_m is defined as

$$\chi_m = \begin{cases} 0, & m \leq 1, \\ 1, & m > 1. \end{cases} \quad (24)$$

It should be noted that $f_m(\eta, \hbar, \beta)$ for $m \geq 1$ is governed by the linear Eq.(22) with boundary conditions (23). Thus, the HAM has efficaciously converted the nonlinear Eq. (8) with relevant boundary conditions into an infinite series of linear sub-problems, which can be solved.

4 Convergence region and the error analysis

As pointed out by Liao [37], the convergence rate and the convergence region of the HAM series solution is strongly tied to the convergence control parameter. Therefore, the optimal solution is obtained vis-à-vis optimal choice of the convergence control parameter. In 2007, Yabushita et al. [38] suggested squared residual error as a means to determine the optimal convergence-control parameter in the framework of the HAM. The exact squared residual error for the m^{th} -order solution is defined as

$$E_m(\hbar, \beta) = \int_0^{\infty} (\mathcal{N}[f_m(\eta, \hbar, \beta)])^2 d\eta. \quad (25)$$

In practice, it is often too computationally demanding to evaluate the integral in (25), even for lower order approximations. Alternatively, we make use of an average squared residual error

$$E_m(\hbar, \beta) = \frac{1}{N+1} \sum_{i=0}^N (\mathcal{N}[\sum_{j=0}^m f_j(\eta_i, \hbar, \beta)])^2, \tag{26}$$

where $\eta_i = i\Delta\eta$, and N is a positive integer.

Notice that the series in (21) gives a family of solutions in two parameters, \hbar and β . We may further reduce computation time by selecting an appropriate value of β and minimizing the error function (26) over one parameter, \hbar . It should be reiterated that the HAM provides considerable freedom in selecting the values of \hbar and β , as to ensure convergence of the series solution. On selecting an appropriate value of β , the reader is referred to Liao [39]. In that work, Liao presents a HAM solution to the Blasius flow problem and finds admissible values of β to be $\beta > \beta_c$, where $\beta \approx 2.5$. For computational purposes, we set $\beta = 3$ and minimize the error function (26) to obtain the optimal value of \hbar .

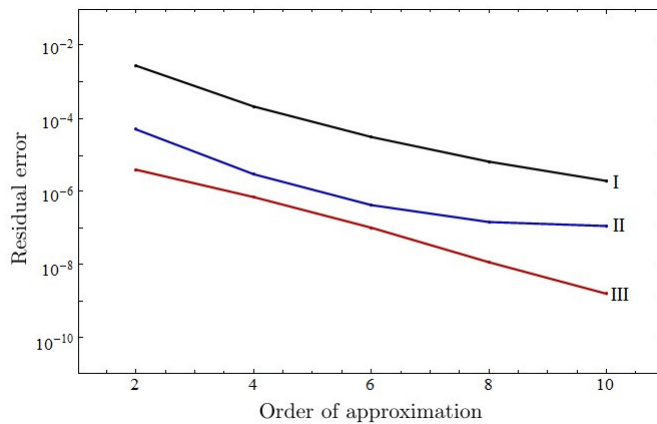


Fig. 2 Average square residual error versus order of approximation for: (I) $Mn = 15, C = 0.001, \lambda_1 = 0.3, \gamma = 1.0,$ and $\delta = -2.0,$ (II) $Mn = 20, C = 0.01, \lambda_1 = 0.2, \gamma = 0.5,$ and $\delta = -0.5,$ (III) $Mn = 10, C = 0.1, \lambda_1 = 0.1, \gamma = 0.1,$ and $\delta = -1.0.$

We consider the following three sets of values for the parameters:

- (I) $Mn = 15, C = 0.001, \lambda_1 = 0.3, \gamma = 1.0,$ and $\delta = -2.0,$
- (II) $Mn = 20, C = 0.01, \lambda_1 = 0.2, \gamma = 0.5,$ and $\delta = -0.5,$
- (III) $Mn = 10, C = 0.1, \lambda_1 = 0.1, \gamma = 0.1,$ and $\delta = -1.0,$

and calculate the 10^{th} -order HAM solution with $\beta = 3$. The optimal values for the convergence control parameter \hbar are found to be, I: $\hbar = -0.17916,$ II: $\hbar = -0.24102,$ and III: $\hbar = -0.30055$. In Fig.2, we presented the average squared residual error against order of approximation for the above three sets of parameters. For the 2^{nd} -order solution, we observed errors of $E_2 = 2.8 \times 10^{-3}, E_2 = 5.0 \times 10^{-5},$ and $E_2 = 3.9 \times 10^{-6}$ for the parametric schemes I, II, and III, respectively. The error decreases as the order of approximation increases, reaching errors of $E_{10} = 1.9 \times 10^{-6}, E_{10} = 1.1 \times 10^{-7},$ and $E_{10} = 1.5 \times 10^{-9}$ for schemes I, II, and III, respectively.

5 Results and discussion

Solutions to the governing Eq. (8) with associated boundary conditions (9) are obtained using the HAM. The mathematical computations were executed using Mathematica 9.0. To confirm the accuracy of the present results, we compare values of the skin friction coefficient $f''(0)$ with numerical (obtained by Runge-Kutta method with shooting technique) and approximate results reported by Vajravelu and Mohapatra [11], for the special case where the magnetic parameter Mn, first-order velocity slip parameter γ , and second-order velocity slip parameter δ are neglected. The results, reported in Table 1, are in excellent agreement. Hence, the outlined solution method in the paper can be applied to the present problem with confidence.

Table 1 Comparison of skin friction coefficient for different values of C and λ_1 in the absence of magnetic parameter Mn, first-order slip parameter γ , and second-order slip parameter δ .

| C | λ_1 | Vajravelu and Mohapatra [11] | | Present work | | |
|------|-------------|------------------------------|-------------|--------------|----------|----------------------|
| | | Numerical | Approximate | HAM | $-\hbar$ | E_{10} |
| 0 | 0 | 0.4698 | 0.4081 | 0.4694 | 1.07698 | 1.8×10^{-4} |
| 0 | -0.4 | 0.3751 | 0.3398 | 0.3751 | 1.06885 | 1.5×10^{-6} |
| 0 | -0.8 | 0.1490 | 0.1411 | 0.1490 | 1.04524 | 2.5×10^{-8} |
| -0.2 | 0 | 0.6190 | 0.5546 | 0.6190 | 1.08715 | 2.2×10^{-5} |
| -0.2 | -0.4 | 0.4578 | 0.4198 | 0.4578 | 1.07285 | 1.7×10^{-7} |
| -0.2 | -0.8 | 0.1757 | 0.1657 | 0.1756 | 1.04966 | 2.7×10^{-9} |

Here we illustrate the effects of the physical parameters on the dimensionless velocity components $f(\eta)$, $f'(\eta)$, and dimensionless shear stress $f''(\eta)$. That is, the effects of magnetic parameter Mn, injection parameter C , velocity ratio parameter λ_1 , first-order velocity slip parameter $\gamma > 0$, and second-order velocity slip parameter $\delta < 0$, are analyzed graphically. Fig.3 shows the f versus η for different values of Mn and C . It can be seen that an increase in Mn or C results in a decrease in f . Additionally, $f(\eta)$ is observed to increase over the entire domain.

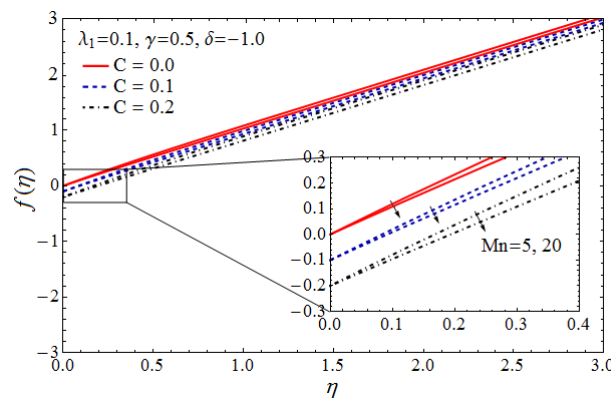


Fig. 3 Similarity profile $f(\eta)$ for various values of Mn and C . The direction of the arrows represents increasing Mn.

The dimensionless velocity and shear stress profiles for different combinations of parameters are displayed in Figs. 4-7. From Figs. 4 and 5, it can be seen that increasing the magnetic parameter Mn has the effect of decreasing the velocity profile, and decreasing the magnitude of the shear stress. Due to an enhanced magnetic field, a Lorentz force is produced opposite to the flow, causing the velocity profile to decrease. The effects of

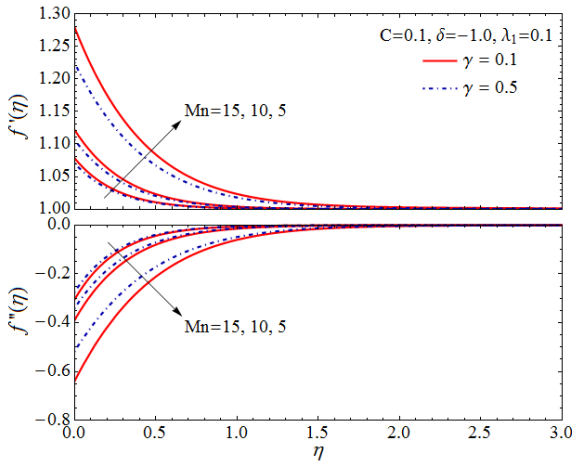


Fig. 4 Dimensionless velocity profile $f'(\eta)$ and shear stress profile $f''(\eta)$ for various values of Mn and γ .

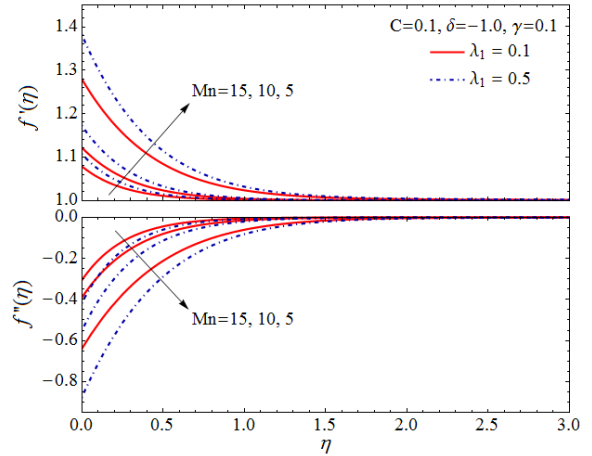


Fig. 5 Dimensionless velocity profile $f'(\eta)$ and shear stress profile $f''(\eta)$ for various values of Mn and λ_1 .

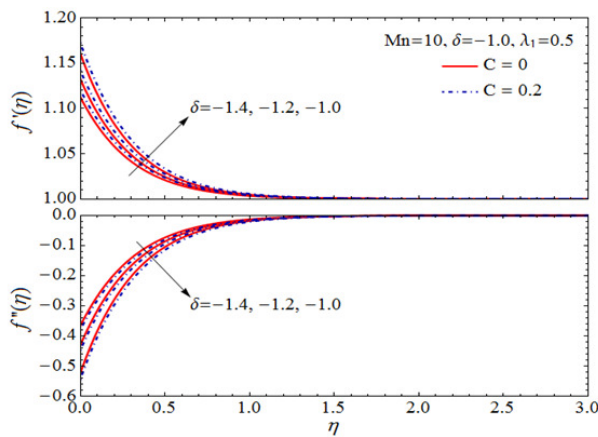


Fig. 6 Dimensionless velocity profile $f'(\eta)$ and shear stress profile $f''(\eta)$ for various values of δ and C .

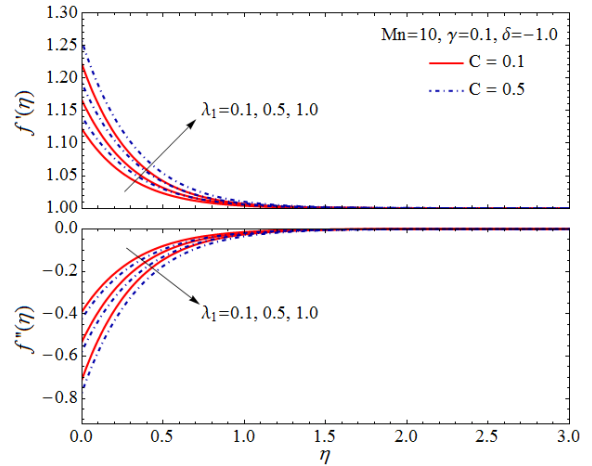


Fig. 7 Dimensionless velocity profile $f'(\eta)$ and shear stress profile $f''(\eta)$ for various values of λ_1 and C .

mass injection parameter C on the velocity and shear stress profiles are displayed in Figs. 6 and 7. From these figures we see that higher velocity and higher magnitude of shear stress occur for larger values of C . Physically, the introduction of mass in to the flow allows the flow to penetrate deeper into the fluid, causing an increase in velocity.

The influence of velocity ratio parameter λ_1 on the velocity and shear stress profiles are shown Figs. 4 and 7. We see that an increase in λ_1 results in an increase in the velocity field and increase in magnitude of the shear stress. From the velocity ratio parameter $\lambda_1 = \frac{U_w}{U_\infty}$, it is interesting to note that the velocity within the boundary layer increases as the free stream velocity decreases (i.e. with increasing values of λ_1 for a constant U_w), thereby causing an increase in the velocity gradient at the surface and increase in skin friction.

The effects of first-order velocity slip parameter γ on the dimensionless velocity and shear stress profiles are displayed in Fig. 4. From this figure, the velocity field and magnitude of the shear stress decrease for increasing values of γ . Fig. 6 depicts the effects of the second-order velocity slip parameter δ on the dimensionless velocity and shear stress profiles. From the figure, we see that the velocity field and magnitude of shear stress decreases with an increase in $|\delta|$.

Table 2 Values of dimensionless skin friction coefficient $-f''(0)$ for different values of Mn, C, λ_1 , γ , and δ .

| λ_1 | γ | δ | Mn | C | $-f''(0)$ | $-\hbar$ | E_{10} |
|-------------|----------|----------|----|-----|--------------|----------|-----------------------|
| 0.1 | 0.1 | -1.0 | 10 | 0.0 | 0.3831367021 | 0.29298 | 1.5×10^{-9} |
| | | | | 0.1 | 0.3901923456 | 0.30055 | 1.5×10^{-9} |
| | | | | 0.2 | 0.3987005677 | 0.32451 | 1.3×10^{-8} |
| | | | 20 | 0.0 | 0.2571008233 | 0.17678 | 3.4×10^{-7} |
| | | | | 0.1 | 0.2602239164 | 0.17830 | 3.1×10^{-7} |
| | | | | 0.2 | 0.2633971893 | 0.17982 | 2.9×10^{-7} |
| 0.1 | 0.1 | -2.0 | 10 | 0.0 | 0.1847004307 | 0.29375 | 2.9×10^{-10} |
| | | | | 0.1 | 0.1880876345 | 0.30028 | 2.8×10^{-10} |
| | | | | 0.2 | 0.1915676774 | 0.32601 | 3.1×10^{-9} |
| | | | 20 | 0.0 | 0.1267106747 | 0.18026 | 9.5×10^{-8} |
| | | | | 0.1 | 0.1281916297 | 0.18175 | 9.0×10^{-8} |
| | | | | 0.2 | 0.1296940688 | 0.18326 | 8.6×10^{-8} |
| 0.1 | 0.5 | -1.0 | 10 | 0.0 | 0.3362198941 | 0.29318 | 1.1×10^{-9} |
| | | | | 0.1 | 0.3420969011 | 0.30025 | 1.1×10^{-9} |
| | | | | 0.2 | 0.3481356753 | 0.32529 | 1.0×10^{-8} |
| | | | 20 | 0.0 | 0.2351151601 | 0.18126 | 4.2×10^{-7} |
| | | | | 0.1 | 0.2377247511 | 0.18272 | 4.0×10^{-7} |
| | | | | 0.2 | 0.2403706095 | 0.18420 | 3.9×10^{-7} |
| 0.2 | 0.1 | -1.0 | 10 | 0.0 | 0.4180362493 | 0.29300 | 1.9×10^{-9} |
| | | | | 0.1 | 0.4263973738 | 0.30067 | 1.9×10^{-9} |
| | | | | 0.2 | 0.4350306454 | 0.32440 | 1.5×10^{-8} |
| | | | 20 | 0.0 | 0.2804874862 | 0.17668 | 4.1×10^{-7} |
| | | | | 0.1 | 0.2838950790 | 0.17819 | 3.8×10^{-7} |
| | | | | 0.2 | 0.2873574604 | 0.17972 | 3.5×10^{-7} |

To further illustrate the effects of the physical parameters on the surface drag force, the dimensionless skin friction coefficient $-f''(0)$ as a function of different pertinent parameters is displayed in Figs. 8-10. As one can see in Fig. 8, the magnitude of the skin friction coefficient increases as λ_1 increases, but decreases with increasing Mn. Fig. 9 shows the skin friction coefficient as a function of γ for two values of C. From Fig. 10, we see that the magnitude of the skin friction coefficient decrease as $|\delta|$ increases. The functional dependence of the skin friction coefficient on C is illustrated in Figs. 9 and 10. It is noticed that the magnitude of skin friction coefficients is lower when there is no fluid injection in to the boundary layer ($C = 0$). Additional values for the dimensionless skin friction coefficient $-f''(0)$ are presented in Table 2. This table further illustrates the effects of the physical parameters on the shear stress at the surface.

6 Conclusions

The viscous flow with second-order velocity slip over a porous moving flat plate subjected to a perpendicular magnetic field is investigated. The governing nonlinear partial differential equation is transformed in to a nonlinear ordinary differential equation by an appropriate similarity transformation. We solved the resulting equation analytically by the homotopy analysis method. The influence of various physical parameters on the velocity field and shear stress are analyzed and discussed. Some of the conclusions are as follows:

- Velocity and shear stress values are lower in the presence of the two slip parameters;
- The presence of mass injection results in higher velocity and skin friction coefficient;

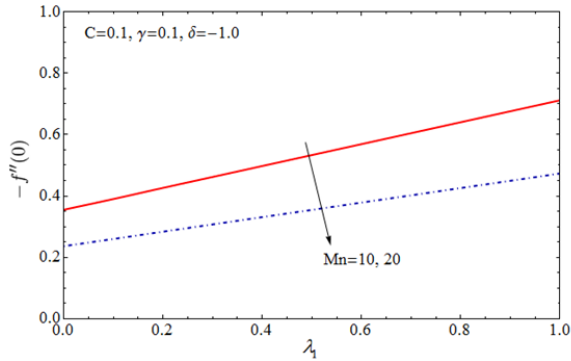


Fig. 8 Dimensionless skin friction coefficient $-f''(0)$ versus λ_1 for different values of Mn.

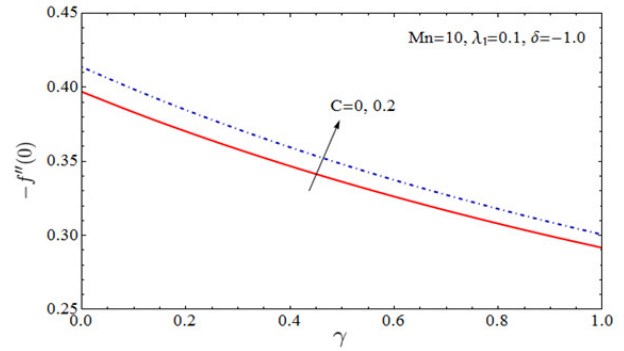


Fig. 9 Dimensionless skin friction coefficient $-f''(0)$ versus γ for different values of C.

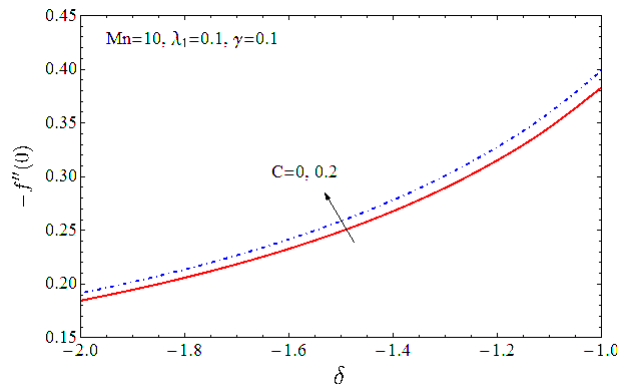


Fig. 10 Dimensionless skin friction coefficient $-f''(0)$ versus δ for different values of C.

- The effect of increasing magnetic parameter is to reduce the velocity field and the shear stress, while the opposite is true with the velocity ratio parameter.

Thus, the inclusion of mass injection and two slip parameters have significant influence on the fluid flow and shear stress at the surface of the moving plate, as well as in the fluid medium.

References

- [1] B.C. Sakiadis, 1. (1961), Boundary layer behaviour on continuous solid surface. I: The boundary layer equation for two dimensional and asymmetric flow, *AICHE J.* 7, 26-28. [10.1002/aic.690070108](https://doi.org/10.1002/aic.690070108)
- [2] B.C. Sakiadis, 2. (1961), Boundary layer behaviour on continuous solid surface. II: The boundary layer on a continuous flat surface, *AICHE J.* 7, 221-225. [10.1002/aic.690070211](https://doi.org/10.1002/aic.690070211)
- [3] H. Blasius, 3. (1908), Grenzschichten in Flüssigkeiten Mit Kleiner Reibung, *Zeitschrift für Mathematik und Physik*, 56, 1-37.
- [4] F.K. Tsou, E. M. Sparrow, J. R. Goldstein, 4. (1967), Flow and Heat Transfer in the Boundary Layer on a Continuous Moving Surface, *International Journal of Heat and Mass Transfer* 10, 219-235. [10.1016/0017-9310\(67\)90100-7](https://doi.org/10.1016/0017-9310(67)90100-7)
- [5] K. Vajravelu and R.N. Mohapatra, 5. (1990), On fluid dynamic drag reduction in some boundary layer flows, *Acta Mech.* 81, 58-68. [10.1007/BF01174555](https://doi.org/10.1007/BF01174555)
- [6] H.S. Takhar, S. Nitu, I. Pop, 6. (1991), Boundary layer flow due to a moving plate: variable fluid properties, *Acta Mechanica* 90, 37-42. [10.1007/BF01177397](https://doi.org/10.1007/BF01177397)
- [7] H. I. Andersson, J.B. Aarseth, 7. (2007), Sakiadis flow with variable fluid properties revisited, *International Journal of Engineering Science*, 45, 554-561. [10.1016/j.ijengsci.2007.04.012](https://doi.org/10.1016/j.ijengsci.2007.04.012)
- [8] S. Ahmad, A.M. Rohni, I. Pop, 8. (2011), Blasius and Sakiadis problems in nanofluids, *Acta Mechanica* 218, 195-204. [10.1007/s00707-010-0414-6](https://doi.org/10.1007/s00707-010-0414-6)

- [9] D. Xu, X. Guo, 9. (2013), Application of fixed point method to obtain semi-analytical solution to Blasius flow and its variation, *Applied Mathematics and Computation* 224, 791-802. [10.1016/j.amc.2013.08.066](https://doi.org/10.1016/j.amc.2013.08.066)
- [10] K. Vajravelu, K. V. Prasad, H. Vaidya, 10. (2016), Influence of Hall Current on MHD Flow and Heat Transfer over a slender stretching sheet in the presence of variable fluid properties, *Communications in Numerical Analysis* 2016, 17-36. [10.5899/2016/cna-00251](https://doi.org/10.5899/2016/cna-00251)
- [11] K. V. Prasad, H. Vaidya, K. Vajravelu, M.M. Rashidi, 11. (2016), Effects of Variable Fluid Properties on MHD Flow and Heat Transfer over a Stretching Sheet with Variable Thickness, *Journal of Mechanics*, 1-12. [10.1017/jmech.2016.101](https://doi.org/10.1017/jmech.2016.101)
- [12] K. V. Prasad, K. Vajravelu, H. Vaidya, 12. (2016), Hall effect on MHD flow and heat transfer over a stretching sheet with variable thickness, *International Journal for Computational Methods in Engineering Science and Mechanics* 17, 288-297. [10.1080/15502287.2016.1209795](https://doi.org/10.1080/15502287.2016.1209795)
- [13] K.V. Prasad, K. Vajravelu, H. Vaidya, 13. (2016), MHD Casson Nanofluid Flow and Heat Transfer at a Stretching Sheet with Variable Thickness, *Journal of Nanofluids* 5, 423-435. [10.1166/jon.2016.1228](https://doi.org/10.1166/jon.2016.1228)
- [14] G.S. Beavers, D.D. Joseph, 14. (1967), Boundary conditions at a naturally permeable wall, *J. Fluid Mech.* 30, 197-207. [10.1017/s0022112067001375](https://doi.org/10.1017/s0022112067001375)
- [15] H. I. Andersson, 15. (2002), Slip flow past a stretching surface, *Acta Mechanica* 158, 121-125. [10.1007/BF01463174](https://doi.org/10.1007/BF01463174)
- [16] C.Y. Wang, 16. (2002), Flow due to a stretching boundary with partial slip - an exact solution of the Navier-Stokes equations, *Chemical Engineering Science* 57, 3745-3747. [10.1016/S0009-2509\(02\)00267-1](https://doi.org/10.1016/S0009-2509(02)00267-1)
- [17] T. Fang, J. Zhang, S. Yao, 17. (2009), Slip MHD viscous flow over a stretching sheet - an exact solution, *Commun. Nonlinear Sci. Numer. Simul.* 14, 3731-3737. [10.1016/j.cnsns.2009.02.012](https://doi.org/10.1016/j.cnsns.2009.02.012)
- [18] M. Sajid, N. Ali, Z. Abbas, T. Javed, 18. (2010), Stretching flows with general slip boundary condition, *Int. J. Mod. Phys. B* 24, 5939-5947. [10.1142/S0217979210055512](https://doi.org/10.1142/S0217979210055512)
- [19] M.T. Matthews, J.M. Hill, 19. (2008), A note on the boundary layer equations with linear partial slip boundary condition, *Appl. Math. Lett.* 21, 810-813. [10.1016/j.aml.2007.09.002](https://doi.org/10.1016/j.aml.2007.09.002)
- [20] T. Hayat, T. Javed, Z. Abbas, 20. (2008), Slip flow and heat transfer of a second grade fluid past a stretching sheet through a porous space, *Int. J. Heat Mass Transfer* 51, 4528-4534. [10.1016/j.ijheatmasstransfer.2007.12.022](https://doi.org/10.1016/j.ijheatmasstransfer.2007.12.022)
- [21] M.H. Yazdi, S. Abdullah, I. Hashim, K. Sopian, 21. (2011), Slip MHD liquid flow and heat transfer over non-linear permeable stretching surface with chemical reaction, *Int. J. Heat Mass Transfer* 54, 3214-3225. [10.1016/j.ijheatmasstransfer.2011.04.009](https://doi.org/10.1016/j.ijheatmasstransfer.2011.04.009)
- [22] B. Sahoo, 22. (2010), Flow and heat transfer of a non-Newtonian fluid past a stretching sheet with partial slip, *Commun. Nonlinear Sci. Numer. Simul.* 15, 602-615. [10.1016/j.cnsns.2009.04.032](https://doi.org/10.1016/j.cnsns.2009.04.032)
- [23] J. Zhu, L. Zheng, L. Zheng, X. Zhang, 23. (2015), Second-order slip MHD flow and heat transfer of nanofluids with thermal radiation and chemical reaction, *Applied Mathematics and Mechanics* 36, 1131-1146. [10.1007/s10483-015-1977-6](https://doi.org/10.1007/s10483-015-1977-6)
- [24] S.Mansur, A. Ishak, I. Pop, 24. (2014), Flow and heat transfer of nanofluid past stretching/shrinking sheet with partial slip boundary conditions, *Applied Mathematics and Mechanics* 35, 1401-1410. [10.1007/s10483-014-1878-7](https://doi.org/10.1007/s10483-014-1878-7)
- [25] J. Zhu, S. Wang, L. Zheng, X. Zhang, 25. (2017), Heat transfer of nanofluids considering nanoparticle migration and second-order slip velocity, *Applied Mathematics and Mechanics* 38, 125-136. [10.1007/s10483-017-2155-6](https://doi.org/10.1007/s10483-017-2155-6)
- [26] B. Sahoo, 26. (2010), Effects of slip, viscous dissipation and Joule heating on the MHD flow and heat transfer of a second grade fluid past a radially stretching sheet, *Applied Mathematics and Mechanics* 31, 159-173. [10.1007/s10483-010-0204-7](https://doi.org/10.1007/s10483-010-0204-7)
- [27] T. Hayat, M. Imtiaz, A. Alsaedi, 27. (2015), Partial slip effects in flow over nonlinear stretching surface, *Applied Mathematics and Mechanics* 36, 1513-1526. [10.1007/s10483-010-0204-7](https://doi.org/10.1007/s10483-010-0204-7)
- [28] J.C. Maxwell, 28. (1879), On stresses in rarefied gases arising from inequalities of temperature, *Philos. Trans. Royal Soc.* 170, 231-256.
- [29] A. Beskok, G.E. Karniadakis, 29. (1999), A model for flows in channels, pipes, and ducts at micro and nano scales, *Microscale Thermophys Eng* 3, 43-77. [10.1080/108939599199864](https://doi.org/10.1080/108939599199864)
- [30] L. Wu, 30. (2008), A slip model for rarefied gas flows at arbitrary Knudsen number, *Appl. Phys. Lett.* 93, 253103. [10.1063/1.3052923](https://doi.org/10.1063/1.3052923)
- [31] T. Fang, S. Yao, J. Zhang, A. Aziz, 31. (2010), Viscous flow over a shrinking sheet with a second order slip flow model, *Commun. Nonlinear Sci. Numer. Simul.* 15, 1831-1842. [10.1016/j.cnsns.2009.07.017](https://doi.org/10.1016/j.cnsns.2009.07.017)
- [32] S.J. Liao, 32. (1992), The proposed homotopy analysis technique for the solution of nonlinear problems, PhD thesis. Shanghai Jiao Tong University Shanghai, China.
- [33] R. A. Van Gorder, K. Vajravelu, 33. (2008), Analytic and numerical solutions to the Lane-Emden equation, *Phys. Lett. A.* 372, 6060 - 6065. [10.1016/j.physleta.2008.08.002](https://doi.org/10.1016/j.physleta.2008.08.002)
- [34] R. Li, R. A. Van Gorder, K. Mallory, K. Vajravelu, 34. (2014), Solution method for the transformed time-dependent Michaelis-Menten enzymatic reaction model, *J. Math. Chem.* 52, 2494-2506. [10.1007/s10910-014-0397-y](https://doi.org/10.1007/s10910-014-0397-y)
- [35] K. Mallory and R. A. Van Gorder, 35, (2014), Optimal homotopy analysis and control of error for solutions to the non-local Witham equation, *Numer. Algorithms.* 66, 843-863. [10.1007/s11075-013-9765-0](https://doi.org/10.1007/s11075-013-9765-0)
- [36] K. Mallory and R. A. Van Gorder, 36. (2013), Control of error in the homotopy analysis of solutions to the Zakharov

- system with dissipation, *Numer. Algorithms.* 64, 633-657. [10.1007/s11075-012-9683-6](https://doi.org/10.1007/s11075-012-9683-6)
- [37] S.J. Liao, 37. (2003), *Beyond perturbation: introduction to the homotopy analysis method*, Boca Raton: Chapman and Hall/CRC Press.
- [38] K. Yabushita, M. Yamashita, K. Tsuboi, 38. (2007), An analytic solution of projection motion with the quadratic resistance law using the homotopy analysis method, *J. Phys. A: Math. Theor.* 40, 8403 - 8416. [10.1088/1751-8113/40/29/015](https://doi.org/10.1088/1751-8113/40/29/015)
- [39] S.J. Liao, 39. (1999), An explicit, totally analytic approximate solution for Blasius' viscous flow problems, *Int. J. Nonlinear Mech.* 34, 759-778. [10.1016/S0020-7462\(98\)00056-0](https://doi.org/10.1016/S0020-7462(98)00056-0)